

Material Characterization Innovations in Microwave Measurement Laboratory of Amirkabir University of Technology

Gholamreza Moradi* 

Department of Electrical Engineering,
Amirkabir University of Technology,
Tehran, Iran
ghmoradi@aut.ac.ir

Received: 5 May 2023 – Revised: 9 August 2023 - Accepted: 27 August 2023

Abstract—This paper presents some microwave circuits, designed for characterization of materials' permittivity. These include single and multiple-resonant types, transmission line approaches, radiation structures and planar circuits. They have either theoretical analysis, simulations, behavior analysis, or fabrication results. A simple half-wavelength coaxial system is used for measuring velocity factor or dielectric constant of the cable. This method presents very accurate results. A planar multi-dielectric antenna structure is proposed whose layers comprise the dielectric under test. The near field as well as the radiation performances are influenced by the permittivity, which is the basis for determining this parameter. Also, a planar resonant cavity is designed and optimized to give enhanced coupling performance and gets higher quality factors. It has a small size and its sensitivity is improved employing a chamfer. The values of dielectric constants are extracted from scattering parameters. In another method, a three-section microstrip line is used whose time domain response is employed to retrieve the dielectric constant. This method can be generalized to other planar lines. At last, a simple method for measuring complex conductivity of lossy planar conductors is studied and it is employed for characterization of a graphene oxide layer.

Keywords: Cable Characteristics, Complex Permittivity, Dielectric Constant, Microwave Measurement, Printed Circuit Measurement, , Substrate Integrated Waveguide, Time Domain Reflectometry.

Article type: Research Article



© The Author(s).

Publisher: ICT Research Institute

I. INTRODUCTION

Microwave measurements have been a growing topic within the recent decades. There are tens of books, published on this subject [1-9]. One of important microwave measurement cases is the electromagnetic identification of materials, which mainly talks on the permittivity, permeability and conductivity. Most of dielectric materials we are working with, are non-magnetic. This means that for each of them, the permeability is the same as permeability of air. So, for typical dielectric materials, the most identifying parameter is permittivity or dielectric constant. There are several methods for measuring this parameter. Some of these methods require complicated test sets.

Characterization of materials is important in many areas, including health care, oil industry, agriculture, and defense applications [9-11]. The high frequency and microwave characterization technics are among the methods providing noninvasive and accurate results. These include free-space propagation methods, planar transmission-line techniques, coaxial probes, and cavity resonator technics [12-18], These methods are based on measuring the multiport circuit parameters in the presence and absence of material under test (MUT). These parameters may be the scattering matrix, impedance, admittance, and hybrid representations.

In another categorization, the measurement technics include resonant and non-resonant ones. The main disadvantages for non-resonant structures are

* Corresponding Author

physical profile and sensitivity. Instead, the resonator-based methods provide high accuracy and less sensitivity to noises during measurements [19-21]. Traditionally, in resonator-based techniques, the main component is metal waveguides. Of course, to overcome the big size, heavy-weight, and inability to be integrated with other planar structures, the metal waveguide is being replaced with its planar counterpart. i.e. the substrate integrated waveguide (SIW).

In resonator-based techniques, cavity perturbation is popular for extracting electromagnetic parameters of materials in microwave bands. However, this method suffers from different assumptions that restricts accuracy. In the recent researches, [22–25], some of these limitations have been relaxed, which in turn have enhanced the sensitivity. Some researchers hire machine learning approaches for identifying the materials based on collected data [25-26]. Artificial neural networks are suitable for reconstructing complex permittivity according to the measured values.

To test the liquids' permittivity using cavity resonators. They are immersed in a large volume of liquid specimens, or their sample holders are filled with samples [24]. An interaction between the liquid and the electric fields is happened, and the scattering parameters reflect this interaction. Therefore, by employing the scattering parameters, dielectric properties of the liquid under test (LUT) are extracted. Such methods, however, suffer from low sensitivity, and a considerable number of specimens is required.

In this work, an SIW sensor is designed and optimized to have a small size. The sensor's sensitivity is enhanced by using internal vias. Also, the proposed sensor's quality factor is enhanced by using the novel tapering feed line. Unlike other works [27-29], which used resonance frequency shift as the input, this work is mainly based on morphology analysis of the scattering parameter. A set of features, including five features, is collected as the input data, and the complex permittivity is considered the output. Also, the proposed sensor has the potential to work under the condition where a small amount of sample is available.

The rest of this paper is organized as follows. The resonator structures for characterization of dielectrics are outlined in Section II. Section III is devoted to the permittivity measurement of a thin layer graphene. Section IV illustrates the sensor design procedure and parametric studies via simulation modeling for the return loss. Section V describes the development of the proposed method in detail. Section VI, talks on employing planar antenna for characterization of dielectrics. Material detection using an array of microwave sensors and machine learning algorithms is reviewed in Section VI. The section VII studies TDR approach for extraction of materials' permittivity. Two-port network approach for permittivity measurement is studied in Section VIII. The last section reviews the main conclusions of this research.

II. RESONATOR STRUCTURES FOR CHARACTERIZATION OF DIELECTRICS

A basic principle says that in function $y = f(x, p)$ where, p is a parameter, one can extract p , by providing some pairs of (x, y) . This rule is crucial in measurement systems. Here it is used to obtain ϵ_r from the transmission line golden rule for the input impedance:

$$Z_{in} = R_0 \frac{Z_L + jR_0 \tan\left(\frac{2\pi cf\sqrt{\epsilon_r}}{l}\right)}{R_0 + jZ_L \tan\left(\frac{2\pi cf\sqrt{\epsilon_r}}{l}\right)} \quad (1)$$

in which, R_0 , Z_L , l , c , and f are respectively, the line's characteristic impedance, load impedance, the line length, celerity of light, and the operating frequency. If the line is terminated to a short circuit impedance, $Z_L = 0$, we get

$$Z_{SC} = jR_0 \tan\left(\frac{2\pi cf\sqrt{\epsilon_r}}{l}\right) \quad (2)$$

By considering this equation as a function of $Z_{SC} = f(\epsilon_r)$, we can derive the value of ϵ_r versus the known parameters in the formula. Here to measure the dielectric constant of a coaxial line, we develop a simple scenario, as shown in Fig. 1. Assume we are to measure ϵ_r at around 100 MHz. By a rough guess of ϵ_r , we calculate the approximate value of the wavelength, i.e. $\lambda = \frac{c}{f\sqrt{\epsilon_r}}$. Then, we choose a half-wave line, i.e. $l = \frac{\lambda}{2}$. Since for a short-circuited half wavelength line, the input impedance and voltage are zero, we anticipate the same for our short-circuited coaxial line. However, this is not the case, because due to that rough approximation, the line length is not exactly a half wavelength. To tackle this, we change smoothly the operating frequency and measure the input voltage. If for a given frequency, the input voltage be zero, the resonant condition is happened and hence:

$$\epsilon_r = \left(\frac{c}{2lf}\right)^2 \quad (3)$$

We performed this test for an RG58U cable and measured the permittivity. The obtained result is $\epsilon_r = 2.23$, which has less than 2% error. Repeating this for a few other cables, we gained the permittivity in the same order of accuracy. This technic, although very simple, has remarkable results for VHF and UHF cables. In our microwave measurement lab, we do these measurements tens of times for each given frequency between 30-1000 MHz. Then, we use the law of large numbers, to get a better estimation of the permittivity. Hence, the error is negligible.

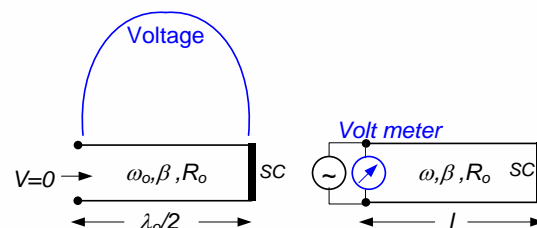


Figure 1. Half wavelength method for cable's permittivity extraction.

The above-mentioned can be generalized, so that another method for characterization of materials can be performed by measuring the phase response of the sample under test. In this method, the source signal is splitted into two paths, where one of them passes through a standard phase shifter and the other one passes through the sample. Then the two output signals are combined to get the unknown permittivity.

III. PERMITTIVITY MEASUREMENT OF A THIN LAYER GRAPHENE

Graphene as a lattice, one-atom thickness, 2D structure with special optical, mechanical, chemical, electronic, and thermal properties that has applications ranging from ultrahigh speed transistors to crystal solar cells [30-33]. Its performance can be controlled by the complex surface conductivity or permittivity. In electromagnetic modeling of lossy materials, complex permittivity and complex conductivity have the same information. Measuring either of these leads to characterizing graphene-based circuits. Mostly, multilayer graphene is used as a bulky structure employed in microwave, mm-wave and Hz circuits.

Here, we introduce an easy routine for measuring the conductivity of the graphene structure, developed in Amirkabir University of Technology. Actually, these thin layer films were fabricated as patch antenna based on graphene oxide, which is thicker and more stable than the pure graphene layer. As shown in Fig. 2, the graphene oxide which is grown on a transparent dielectric slab or substrate plays the role of a transmission line terminated by a high impedance substrate. Although the impedance of the substrate is finite, it is seen as an open circuit. This is because the graphene's impedance is much smaller than that of the holder. To analyze this structure, consider the well-known impedance equation (Z_{in}), versus the characteristic impedance, (Z_0), load impedance (Z_L), the propagation constant (γ), and the line's length (l), as:

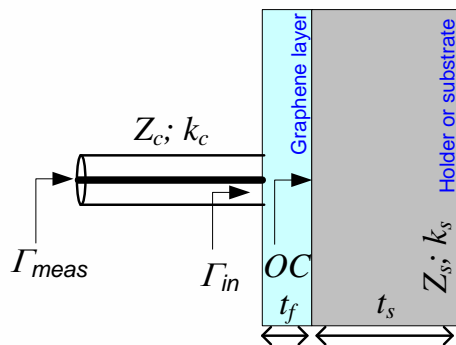


Figure 2. Measurement setup for graphene's conductivity extraction.

$$Z_{in} = Z_0 \frac{Z_L + Z_0 \tanh(\gamma l)}{Z_0 + Z_L \tanh(\gamma l)} \quad (4)$$

For an open circuit load, we get:

$$Z_{in} = \frac{1}{Y_0 \tanh(\gamma l)} \approx \frac{1}{Y_0 \gamma l} \quad (5)$$

where, the last equality is due to the small value of γl . Since we have $Y_0 \gamma = \sigma + j\omega \epsilon$, and $l = t_f$, we will obtain

$$\sigma + j\omega \epsilon \approx \frac{1}{t_f Z_{in}} \quad (6)$$

in which, t_f is the graphene's thickness. On the other hand, the input impedance can be expressed versus the reflection coefficient (Γ_{in}), and cable's dielectric constant (ϵ_r) as:

$$Z_{in} = \frac{\eta_0}{\sqrt{\epsilon_r}} \frac{1 + \Gamma_{in}}{1 - \Gamma_{in}} \quad (7)$$

Therefore, by combining (6) and (7), we get:

$$\sigma = \frac{1}{\eta_0 t_f} \text{Re} \left[\sqrt{\epsilon_r} \frac{1 - \Gamma_{in}}{1 + \Gamma_{in}} \right] \quad (8)$$

Once we measure the input impedance or reflection coefficient by using a network analyzer, all parameters in this equation are known. In mm-wave laboratory of Amirkabir University of Technology, we measured Γ_{in} in 50-2000 MHz, and extracted the conductivity and the refractive index of the graphene, as shown in Fig. 3. The reported refractive index of the layer in UHF band is around 35 which verifies our measurement result. Also, the conductivity is close to the fabricator's data.

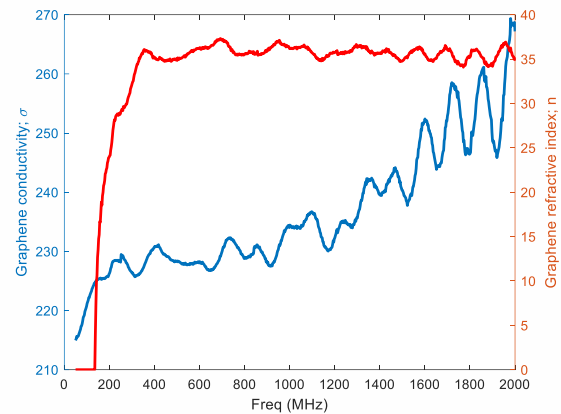


Figure 3. Measured values of conductivity and refractive index of the graphene.

In another version of this test, if there be no substrate or holder, we can calculate the complex permittivity as:

$$\sigma + j\omega \epsilon \approx \frac{1}{t_f \eta_0} \left(\frac{\eta_0 + j\omega t_f}{Z_{in}} - 1 \right) \quad (9)$$

The above-mentioned routine can be similarly employed in measuring the characteristics of other thin layer structures. This can be done for characterizing complex conductivity, complex permittivity, refraction index, loss tangent and velocity factor of lossy thin conductors.

IV. EMPLOYING PLANAR ANTENNA FOR CHARACTERIZATION OF DIELECTRICS

Planar antennas use one or several dielectric substrate layers. The antenna performance is affected by the permittivity of the substrates [34-36]. We designed a multi-layer microstrip antenna in which one of the layers is a liquid, as shown in Fig. 4a. Different liquids lead to different radiation characteristics. Here in this research, we do a reverse approach. We measure

antenna parameters and use them in measuring the liquid's permittivity. It must be noted that we can equivalently use inverted microstrip as shown in Fig. 4b. The measurement set-up is a conventional one. Fig. 5 shows the near field measurement set up, and Fig. 6 gives the measured as well as the simulated response. Using these data, and employing a commercial simulator, one can determine the permittivity of the liquid under test. It is straightforward to prepare a look up table to relate the permittivity to the antenna radiation parameters. This method can be generalized to other types of planar antennas. Here, this method is applied to a mixture of different liquids, and the obtained results are promising. One should note that mixtures of liquids are used in polymer industry, pharmaceutical companies, and oil factories.

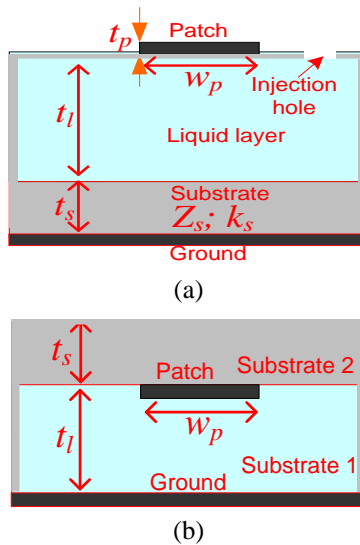


Figure 4. Antenna approach for permittivity measurement, (a) microstrip (b) inverted microstrip.

V. CAVITY RESONATOR SENSORS FOR CHARACTERIZATION OF DIELECTRICS

Cavity resonators can be used in determining dielectric constant of materials. In this method, the variation in resonant frequency and bandwidth or quality factor of the cavity is used as a measure for calculating the resonator's response. The transmission structure can be strip line, microstrip, coplanar strips, coplanar waveguide, or other planar lines. Here we use SIW cavity for which, we know [26, 37]:

$$\epsilon_r = 1 + \frac{V_c}{2V_s} \left(\frac{f_0 - f}{f} \right) + j \frac{V_c}{4V_s} \left(\frac{1}{Q} - \frac{1}{Q_0} \right) \quad (10)$$

where f_0 , f , Q_0 , and Q are the resonant frequency and quality factor of an empty and filled cavity, respectively. C represents the shape factor coefficient while V_s and V_c are the sample and the cavity volumes, respectively. It should be mentioned that SIWs combine the compactness advantage of planar technologies, and high quality factor of conventional waveguides [38-40].

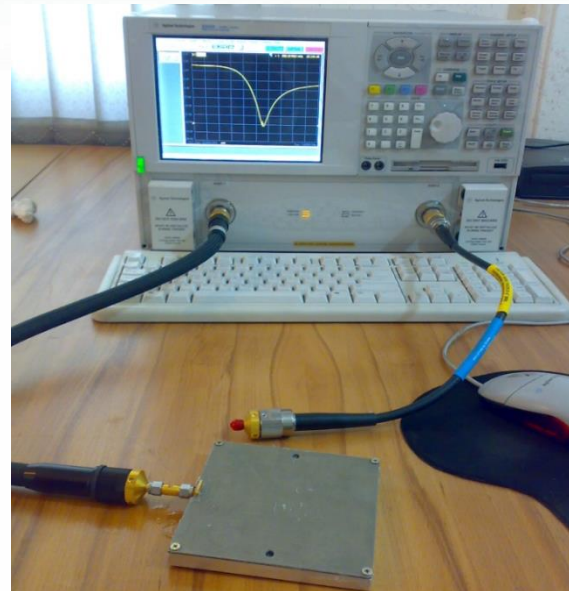


Figure 5. The Agilent network analyzer used for measuring return loss of inverted patch resonator

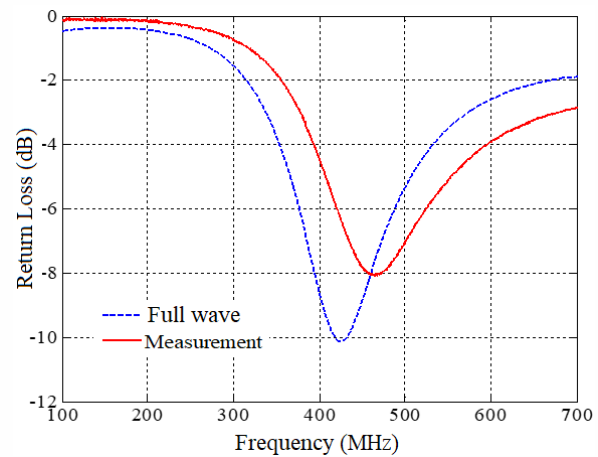


Figure 6. Measurement (dashed) versus simulated (solid) data for inverted patch resonator, with 30-70% ethanol-methanol mixture as the liquid under test.

The detailed geometry of the SIW structure is illustrated in Fig. 7. The microwave sensor is designed on a double-layer substrate of Rogers 4003 with permittivity and loss tangent of $\epsilon_r = 3.55$ and $\tan\delta = 0.0027$, respectively, and a thickness of 1.6 mm. The selection of SIW structure is based on its low cost, easy fabrication, low radiation features, and more importantly, the capability of integration with other planar circuits. The resonant frequency in SIW is determined by effective width and length, as shown in the following equations [23]:

$$f_{mno} = \frac{c}{2\pi\sqrt{\epsilon_r}} \sqrt{\left(\frac{m}{a_{\text{eff}}}\right)^2 + \left(\frac{n}{b_{\text{eff}}}\right)^2} \quad (11)$$

where the m and n are the mode indices, ϵ_r represents the relative permittivity of the dielectric, respectively. The a_{eff} and b_{eff} are the effective length and width calculated according to the semi-empirical formulas [26].

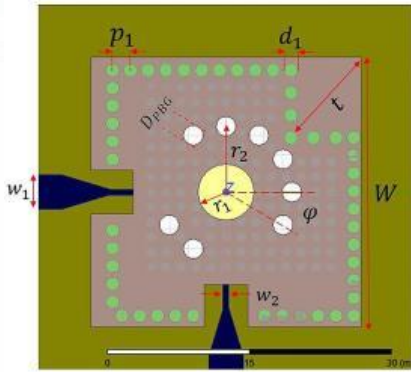


Figure 7. Layout of the SIW sensor [26].

The sensor architecture is developed through several steps. First, a perturbation by some square corner cut is added to the structure. Then an array of holes is added to the sensor design to increase the concentration of electric field through wave encapsulation. In the next step, several rows of metalized vias are embedded in the lower substrate layer to reduce the sensor’s size. Finally, by optimizing the diameter of MUT, the maximum amount of sensitivity is achieved.

The dimensions of the proposed structure are $W = 26$ mm, $t = 4.5$ mm, $w_1 = 3.65$ mm, $w_2 = 0.6$ mm, $p_1 = 2.4$ mm, $d_1 = 1.4$ mm, $r_1 = 3$ mm, $r_2 = 7$ mm and these values are optimized to achieve the minimum return loss. The feedline of the sensor is a 50Ω microstrip, which is matched to the structure using tapered microstrip to SIW transition. This step is done to achieve a higher quality factor and to excite the cavity in under-coupled mode, which is suitable for permittivity extraction.

Simulations are performed using a full wave software, i.e. HFSS. In the first step, the effect of adding vias is studied, and based on this effect, the total size of the sensor is reduced. Then impact of the presence and absence of holes, and the diameter and location of these holes are parametrically studied for the highest sensitivity. Following this step, the corner of the cavity is perturbed by creating a square cut, and it is shown that this technique enhances the concentration of the electric field in the center of the sensor. Finally, the diameter of the MUT is varied to achieve the highest sensitivity.

The MUT should be placed at the region where the electric field concentration is high, to achieve higher sensitivity. By displacing the corner vias as a corner cut, the intensity of the electric field in the corner is squeezed into the center, and therefore, the higher electric field intensity is achieved in the center, where the MUT is located. If we simulate the reflection coefficient of the SIW sensor for several values of permittivities and loss tangents., sharp notches are generated when the sample holder is empty, or filled by air.

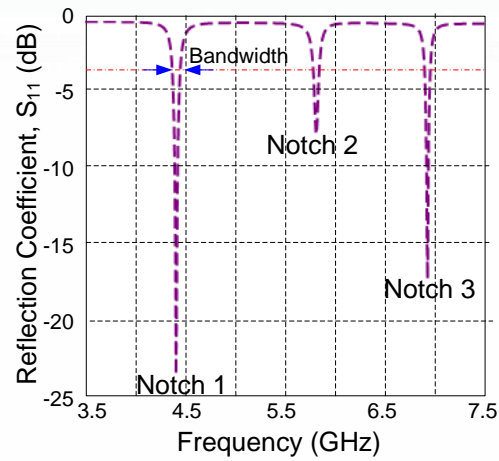


Figure 8. Simulated value of S_{11} of the SIW sensor.

As a thorough survey, a set of different features, including the frequency resonance, the magnitude of scattering parameter, 3-dB bandwidth, quality factor, and the coupling coefficient, can be extracted from the scattering parameters.

To examine the accuracy of the network in the proposed sensor, different mixture of cyclohexane and water is used as a sample. In this study, the two liquids’ complex permittivities are calculated from the first-order Debye model [26, 41].

$$\epsilon^* = \epsilon'(\omega) - j\epsilon''(\omega) = \frac{\epsilon_l + j\omega\tau\epsilon_h}{1 + j\omega\tau} \quad (12)$$

where ϵ_h is the permittivity at the infinite frequency, ϵ_l is the static permittivity, ω is the angular frequency, τ is the relaxation time. In this research, the water is considered as the base liquid and the cyclohexane percentage is varied. Then, the complex permittivity of the mixture is calculated using the widely used binary approximate formula, i.e. $\epsilon_{\text{eff}} = \epsilon_1 f_1 + \epsilon_2 (1 - f_1)$, or the Maxwell-Garnet [26] relation:

$$\epsilon_{\text{eff}} = \epsilon_1 + \frac{2\epsilon_1 + \epsilon_2 + 2f_1(\epsilon_2 - \epsilon_1)}{2\epsilon_1 + \epsilon_2 - f_1(\epsilon_2 - \epsilon_1)} \quad (13)$$

where, ϵ_{eff} is the effective permittivity of the mixture and f_1 is the volume fraction of the cyclohexane. The variation of the mixture relative permittivity (ϵ_r) and the loss tangent is illustrated in Fig. 9. As it can be seen from Fig. 9a, variation of the relative permittivity for different volume ratio starts from that of water and finally reaches to that of cyclohexane. Moreover, in this figure, the approximation obtained from (13) are presented. Fig. 9b is a similar test for another mixture, to reconfirm the method.

It is worth mentioning that by increasing the volume ratio of cyclohexane, the resonance frequency was decreased. This phenomenon can be explained by resonance frequency expression in cavities. According to equation (11), the higher the permittivity, the lower the resonance frequency will be. In addition, in our sensor, the increase in permittivity causes growth in both coupling factor and 3-dB bandwidth. Moreover, our analysis shows the maximum relative permittivity, and the loss tangent errors are less than 2.5%, and 0.6%, respectively.

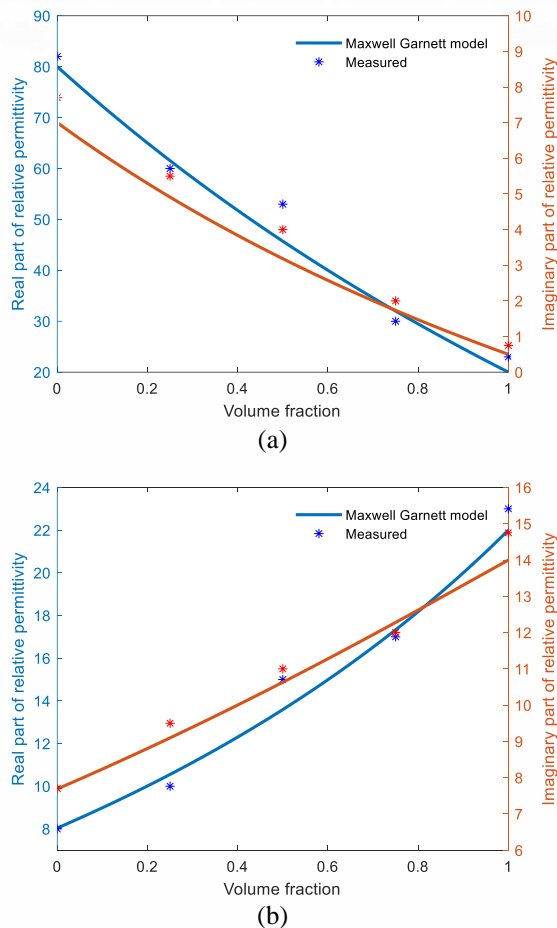


Figure 9. Permittivity of (a) water-cyclohexane mixture for different volume fractions, (b) methanol-ethanol for different volume fractions at 2.4 GHz.

It should be noted that this sensor is smaller than other similar sensors. Meanwhile, the sensitivity of this design is higher. Consequently, it can discriminate close permittivity values. Moreover, in terms of accuracy, this method gets higher value of accuracy.

VI. MATERIAL DETECTION USING AN ARRAY OF MICROWAVE SENSORS AND MACHINE LEARNING ALGORITHMS

With increasing trend of smartening in industries, machine learning algorithms are widely used and their various applications are studied. One of these cases is to identify a material and characterize its different physical properties of materials such as humidity, temperature, etc. In our research, we used the neural network algorithm to increase the accuracy of intelligent material detection [41-43]. Also, in the stage of creating the simulated data, physical properties of materials such as temperature and humidity are affected, which indicates the high efficiency of the model in its application in different climatic conditions. The main steps of the project are:

1. Designing the desired structure in HFSS
2. Creating a set of data to apply machine learning algorithms
3. Implementing machine learning algorithm.

In general, in microwave sensors and spectroscopy systems, the goal is to describe the spectral behavior of materials in the desired frequency range, which can be used to create a systematic low-cost system for detecting material and describing the properties of materials.

In the sensor structure of this material description system, single-resonator structures or a transmission line structure can be used. However, single resonant sensor structures show high sensitivity when exposed to the studied materials. Although this high sensitivity is related to only one finite frequency band, if the test materials have similar properties in the desired resonance bandwidth, these materials will not be distinguished from each other correctly. On the other hand, transmission line-based sensors are suitable for sensor operation at a wide bandwidth but are less sensitive. Given the above, dealing with the exchange between sensitivity and bandwidth to achieve a broadband detection system is challenging. For this reason, in this research, we use a material detection system based on an array of microwave sensors [26, 43], each of them has a different resonant frequency, so that these resonant frequencies cover the desired bandwidth. The result of using combination of transmission lines and resonant elements is to get the high sensitivity of single resonator with high quality factor, and perform the sensor operation in a wide frequency band. The designed structure is shown in Fig. 10.

The values of the distance from the center to the center of the sensors are $x_1 = 11$ mm, $x_2 = 13$ mm, $x_3 = 10$ mm, $x_4 = 8$ mm, $x_5 = 8$ mm, and $x_6 = 6$ mm. The values of the design parameters of each of the five desired CSRR sensors, borrowed from [21], are given in Table 1.

TABLE I. THE VALUES OF THE PARAMETERS OF EACH OF THE FIVE SENSORS, $a = b = 0.16$ MM.

Sensor	f_r (GHz)	W (mm)	L (mm)
1	1.36	0.27	10.5
2	3.09	0.27	5.15
3	5.00	0.27	3.65
4	6.82	0.27	3.00
5	8.91	0.54	3.00

To do the experiment, we put the dielectric under test over the structure. By measuring the transmission scattering parameter of the structure, one can determine the complex permittivity of the sample under test. However, we need some known materials for training the machine learning phase of the algorithm. The datasets are created to apply machine learning algorithms. We know that the wider the data set, the higher the accuracy and more reliable models in practical applications. This set of data can be created in two ways:

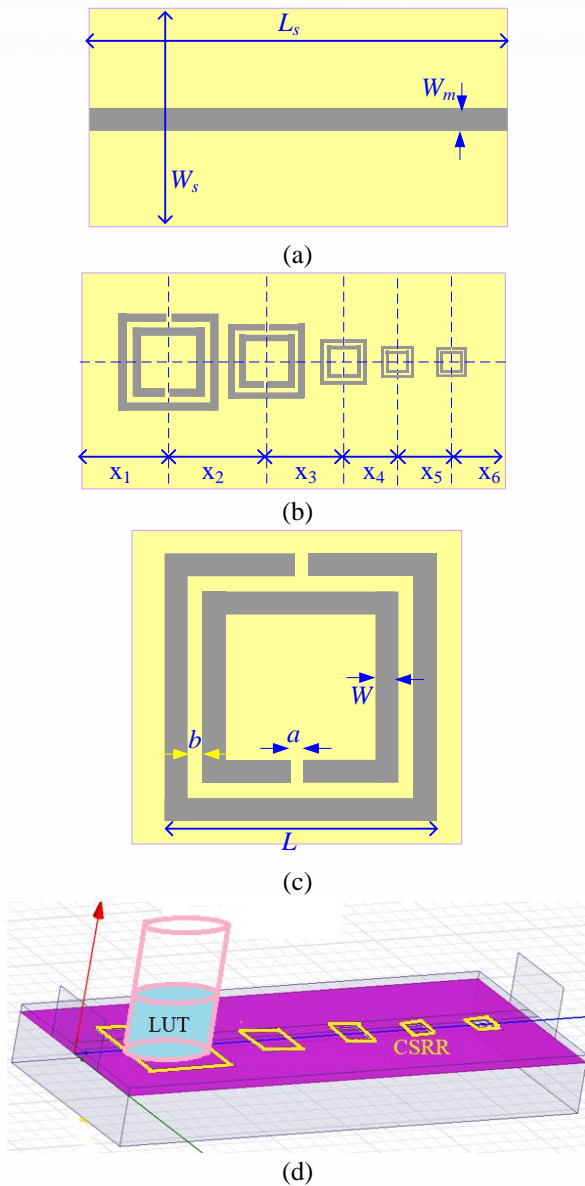


Figure 10. The structure of the substrate. (a) A thin conductive strip on front layer. (b) The structure of five CSRR sensors etched on the ground. (c) The detailed layout of each of five sensors. (d) The designed structure in HFSS.

1. Implement the structure and apply this structure on samples of different materials and record the results.
2. Design the desired structure in the full wave software and then simulate the results of samples of each material.

After training the network with scattering parameters of some known materials, we provided an algorithm for identifying the permittivity of some materials under test.

We did the scenario for some materials. As expected, the method can even discriminate between two species of wood having different humidity contents. This achievement is due to multi-resonance nature of the method, that increases the information. This method may have applications such as industrial liquid identification and composite material identification.

VII. TDR APPROACH FOR EXTRACTION OF PERMITTIVITY

In quasi-TEM transmission systems, dispersion is negligible. Hence, having the temporal functionality of the signals, gets their spatial functionality [44-45]. As a simple and common case, in a 1D transmission lines, the signal traveling in z-direction can be expressed as $y(t) = f(z - vt)$. So, if we measure the frequency response of reflection coefficient of a transmission line, and convert it to the time domain, we get $f(z - vt)$. Now using the spatial map of the line, we can determine the velocity of the propagation. From there, $\epsilon_r = \left(\frac{c}{v}\right)^2$. Using this, we performed this scenario for a simple microstrip-based transmission line, as shown in Fig. 11, and determined the PCB's permittivity. The error was less than 10%. Fig. 12 shows, the time domain reflection response of the circuit, both by simulation and by measurement. As seen, the measured values follow the simulation result obtained by a full wave simulator. It should be noticed that the most existing circuit and full wave simulators e.g. ADS, HFSS and CST presents time domain responses for all scattering parameters.

Time domain reflectometer systems can also be used for modeling and characterization of microwave integrated circuit [46-48].

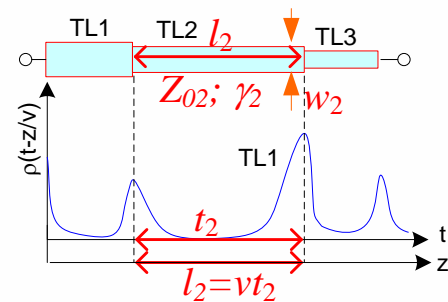


Figure 11. The equivalence in temporal and spatial functionality of a TEM line.

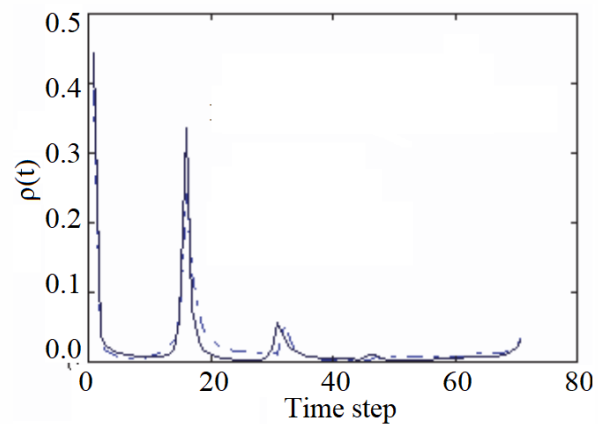


Figure 12. Measurement (dash) versus simulated (solid) TDR results for a transmission line: $d = 15$ cm and $\epsilon_r \approx 3.5$.

VIII. TWO-PORT NETWORK APPROACH FOR PERMITTIVITY MEASUREMENT

Two-port linear microwave circuits can be characterized by impedance, admittance, hybrid, transmission and scattering parameters. Having each of these representations for a transmission line, gives its dielectric's permittivity. Just as a case study, consider, we have measured the distance matrix of a transmission line:

$$Y = \begin{bmatrix} Y_d \coth(\gamma_d l_d) & -Y_d \operatorname{cosech}(\gamma_d l_d) \\ -Y_d \operatorname{cosech}(\gamma_d l_d) & Y_d \coth(\gamma_d l_d) \end{bmatrix} \quad (14)$$

in which, Y_d , γ_d and l_d are the characteristic admittance, propagation constant and length of the transmission line, as shown in Fig. 13. The subscript d refers to the dielectric. Using (14), we get:

$$Y_{11}^2 - Y_{12}^2 = Y_d^2 \quad (15)$$

which means that by measuring Y_{11} and Y_{12} , we have Y_d . If the transmission medium is a TEM one, we have $Y_d^2 = \epsilon_r Y_0^2$, where Y_0 is the characteristic admittance of the hollow line. From there, we get:

$$\epsilon_r = \epsilon_r' - j\epsilon_r'' = \frac{Y_{11}^2 - Y_{12}^2}{Y_0^2} = y_{11}^2 - y_{12}^2 \quad (16)$$

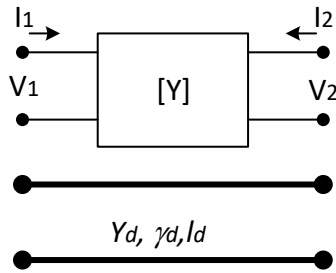


Figure 13. A transmission line and its equivalent admittance representations.

On the other hand, if the transmission medium is a non-TEM one, e.g., a rectangular waveguide, we get:

$$\epsilon_r = \frac{y_\epsilon + \left(\frac{\lambda_g}{\lambda_c}\right)^2}{1 + \left(\frac{\lambda_g}{\lambda_c}\right)^2} \quad (17)$$

in which $y_\epsilon = \frac{Y_{11}^2 - Y_{12}^2}{Y_0^2}$, λ_g is the guide wavelength, and λ_c is the cutoff wavelength. To derive more straightforward relations, we design a setup as Fig. 14.

In this setup, we determine the minimum voltage points in hollow as well as dielectric-filled lines, as shown in Fig. 14. Now, due to resonant condition, we have:

$$Z_0 \tan(\beta l_0) = -Z_d \tan(\beta l_d) \quad (18)$$

and, from there:

$$Z_0 \tan(\beta[l_0 - l_d]) = Z_d \tan(\beta l_d) \quad (19)$$

from where, due to $Z_0 \beta = Z_d \beta_d$, we get

$$\frac{\tan(\beta[l_0 - l_d])}{\beta l_d} = \frac{\tan(\beta l_d)}{\beta_d l_d} \quad (20)$$

This is a useful formula for determining β_d , which easily leads to ϵ_r . We arranged a WR90 waveguide set in microwave lab of Tehran Polytechnic University and measured permittivity of some alcoholic liquids. The results are promising, which is due to the resonant nature of the method. Based on this method, we measured the permittivity of vegetable oil as $\epsilon_r =$

$2.71 - j0.05$ in the mid-band of WR90 waveguide which is around 9.3 GHz. The reported data shows less than 5% error for each of the real and imaginary parts of the permittivity. In another case study, we measured the parameters of transformer oil. The data were $\lambda_g = 1.76''$, $\lambda_c = 1.8''$, $l_d = 0.45''$, $l_0 = 0.18''$, $l_0 + l_d = 0.69''$. Using the former equation, we obtain $\epsilon_r = 2.03$, which is quite close to what we did with transmission line approach.

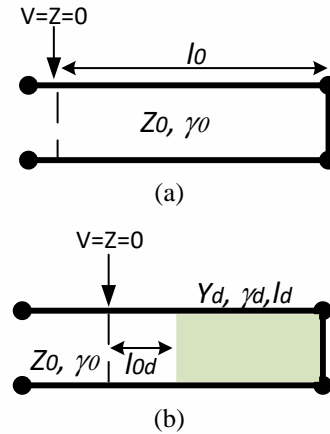


Figure 14. A setup for measuring secondary parameters of a transmission line. (a) Hollow line, (b) dielectric-filled line.

It is important to note that we do not trust to the data sheets, because the different edible oil companies produce different qualities for their products. This means that, to be sure about the accuracy of our method, we must provide a more valid reference. Probably, the best one is a dielectric assessment kit such as Agilent DAK-1.2E-TL2 system.

IX. PERTURBATIONAL METHODS FOR DETERMINING THE RELATIVE PERMITTIVITY

In engineering mathematics terminology, "perturbation" refers to a small change w.r.t. a regular and simple problem. The same is valid for perturbed structures. Therefore, the cavity resonator perturbation is a cavity whose dimension or material slightly differs from a regular one. These two classes are shown in Fig. 15. An approximate perturbational analysis is carried on the structure to relate the resonant frequency of the perturbed system to that of unperturbed one. The formulation is available in the literature for elementary structures [25]. For a custom design, one can extract the necessary equations.

Cavity perturbation methods are very suitable techniques for the measurement of the dielectric constant of materials at microwave frequencies. These methods are important for the cases where the shape of perturbing material is complicated or irregular. We did this for measuring permittivity of a piece of fat, transformer oil, vegetable oil, and plastic at X band, using a WR90 system. Putting the material under test, in the hollow cavity, slightly changes the resonant frequency of the resonator. Then, using the following equation, we determined the desired parameter.

$$\epsilon_r = 1 + \frac{2}{F} \frac{\omega_{r1} - \omega_{r2}}{\omega_{r2}} + j \frac{1}{F} \left(\frac{1}{Q_{T2}} - \frac{1}{Q_{T1}} \right) \quad (21)$$

where F is the filling factor and depends on size and location of the sample in the cavity. The equations for this parameter are available in the literature [25-26]. ω_r and Q_T the resonant angular frequency and the overall quality factor, respectively. Indices 1 and 2, refer to unperturbed and perturbed structures, respectively. This test is currently a part of our microwave measurement course program at the Tehran Polytechnic University. Some typical test results are shown in Table 2. The error value for the real and imaginary parts of the species are respectively less than 5 and 10%. The ease of the method, and the potential to test small samples of materials, and moderate accuracy are some specifications of this method. It is noticeable that to test the liquids, we pour them in a transparent thin box.

TABLE II. COMPLEX PERMITTIVITY OF SOME MATERIALS MEASURED USING THE X BAND WAVEGUIDE TEST SET.

	ϵ_r'	ϵ_r''
Glass	4.79	0.03
Rubber	2.51	0.01
Edible oil	2.76	0.06

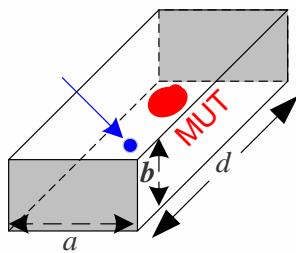


Figure 15. A perturbed cavity resonator in rectangular waveguide system.

X. CONCLUSIONS

In this paper, we analyzed and designed some planar as well as bulky microwave sensors to extract the complex permittivity of materials. Simulations were conducted in full-wave or circuit software. Design steps were discussed in detail. Our results indicate that the studied complex permittivity detection methods were precise and accurate for a wide range of permittivity values.

The reviewed technics show encouraging results of the methods' performances. However, our methods were restricted to some features extracted from the scattering parameters. They can be generalized to extract other features such as phase information to improve accuracy of the results.

A simple method for characterization of the lossy conductive films has been introduced which is versatile and applicable to other similar cases.

A double layer microstrip resonator has been designed and fabricated for characterization of liquids. Permittivity of mixtures of two alcohol liquids having

different volume fractions have been measured with the designed circuit. The simulation results were in well match with the measurement results, i.e., the errors were negligible. Hence, these promising results show that the studied circuits can be a basis for other studies and also, they can help us in providing industrial characterization setups.

The mentioned methods for permittivity measurements can be done for different values of parameters e.g., frequency, temperature, humidity, and density. In this way, one can extract the functionality of dielectrics constant with respect to each of these parameters.

REFERENCES

- [1] R.J. Collier, and A.D. Skinner, "Microwave Measurements (Materials, Circuits and Devices)," IET Press, 3rd Edition, 2007.
- [2] A. Basu, "Introduction to Microwave Measurements," CRC Press; 2014.
- [3] M. Sucher, J. Fox, and M. Wind, "Handbook of Microwave Measurements," Polytechnic Press, 1963
- [4] R. F. Harrington, "Time-Harmonic Electromagnetic Fields," Wiley Interscience, 2001.
- [5] G. H. Bryant, "Principles of Microwave Measurements," IET Press, 3rd Edition, 1993.
- [6] J. P. Dunsmore, "Handbook of Microwave Component Measurements: With Advanced VNA Techniques," Wiley, 2012.
- [7] N. Ida, "Microwave NDT," Springer, 1992.
- [8] L. F. Chen, C. K. Ong, C. P. Neo, V. V. Varadan, Vijay K. Varadan, "Microwave Electronics: Measurement and Materials Characterization," Wiley, 2007.
- [9] A. E. Bailey, "Microwave Measurements," IEE Press, 1980.
- [10] L. Changjun, and P. Yang, "A microstrip resonator with slotted ground plane for complex permittivity measurements of liquids," IEEE Microw. Wireless Compon. Lett, vol. 18, no. 4, 257-259, 2018.
- [11] A.K. Verma, Nasimuddin and A.S. Omar, "Microstrip resonator sensors for determination of complex permittivity of materials in sheet, liquid and paste forms," IEE Proc. Microw. Antennas Propag. vol. 152, no. 1, 48-54, 2005.
- [12] J. Hinojosa, K. Lmimouni, S. Lepilliet, and G. Dambrine, "Very high broadband electromagnetic characterization method of film-shaped materials using coplanar waveguide," Microw. Opt. Technol Lett, vol. 33, 352-355, 2020.
- [13] Z. Bao, M. L. Swicord, and C. Davis, "Microwave dielectric characterization of binary mixtures of water, methanol, and ethanol," Journal of Chemical Physics, vol. 104, 4441-4450, 1996.
- [14] S. Trablsi and S. O. Nelson, "Microwave sensing of quality attributes of agricultural and food products," IEEE Instrum. Meas. Mag., vol. 19, no. 1, pp. 36-41, Feb. 2016.
- [15] Z. Akhter and M. J. Akhtar, "Free-space time domain position insensitive technique for simultaneous measurement of complex permittivity and thickness of lossy dielectric samples," IEEE Trans. Instrum. Meas., vol. 65, no. 10, pp. 2394-2405, Oct. 2016.
- [16] S. Subbaraj, V. Ramalingam, M. Kanagasabai E. Sundarsingh, Y. Selvam, and S. Kingsley, "Electromagnetic nondestructive material characterization of dielectrics using EBG based planar transmission line sensor," IEEE Sensor J., vol. 16, no. 19, pp. 7081-7087, Oct. 2016.
- [17] Y. J. Cheng and X. L. Liu, "W-band characterizations of printed circuit board based on substrate integrated waveguide multi-resonator method," IEEE Trans. Microw. Theory Techn., vol. 64, no. 2, pp. 599-606, Feb. 2016.
- [18] J. Cai, Y. J. Zhou and X. M. Yang, "A metamaterials-loaded quarter mode SIW microfluidic sensor for microliter liquid characterization," J. Electromagn. Wave, vol. 33, no. 3, pp. 261-271, Nov. 2018.

- [19] D. Deslandes and K. Wu, "Integrated microstrip and rectangular waveguide in planar form," *IEEE Microw. Wireless Compon. Lett.*, vol. 11, no. 2, pp. 68–70, Feb. 2001.
- [20] H. B. Wang and Y. J. Cheng, "Broadband printed-circuit-board characterization using multimode substrate-integrated-waveguide resonator," *IEEE Trans. Microw. Theory Techn.*, vol. 65, no. 6, pp. 2145–2152, Jun. 2017.
- [21] N. K. Tiwari, A. Jha and P. Varshney, "Generalized multimode SIW cavity-based sensor for retrieval of complex permittivity of materials," *IEEE Trans. Microw. Theory Techn.*, vol. 66, no. 6, pp. 3063-3072, Jun. 2018.
- [22] A. K. Jha and M. J. Akhtar, "A generalized rectangular cavity approach for determination of complex permittivity of materials," *IEEE Trans. Instrum. Meas.*, vol. 63, no. 11, pp. 2632–2641, Nov. 2014.
- [23] Harrision, L., Ravan, M., Tandel, D., Zhang, K., Patel, T., & K. Amineh, R., "Material Identification Using a Microwave Sensor Array and Machine Learning. Electronics," *MDPI*, vol. 9(2), 288. doi:10.3390/electronics9020288, 2020.
- [24] P. K. Varshney, N. K. Tiwari and M. J. Akhtar, "SIW cavity based compact RF sensor for testing of dielectrics and composites," *IEEE MTTs International Microwave and RF Conference (IMaRC)*, New Delhi, pp. 1-4, 2016.
- [25] K. Kazemi, G. Moradi and A. Ghorbani, "Employing higher order modes in broadband SIW sensor for permittivity measurement of medium loss materials," *Int. J. Microw. Wireless. Technol.*, pp. 1-13, Oct. 2020.
- [26] K. Kazemi, and G. Moradi, "Employing Machine Learning Approach in Cavity Resonator Sensors for Characterization of Lossy Dielectrics," *International Journal of Information and Communication Technology Research.*, vol. 13, no. 3, pp. 1-11, September 2021.
- [27] M. Saadat-Safa, V. Nayyeri, A. Ghadimi, M. Soleimani and O. M. Ramahi, "A pixelated microwave near-field sensor for precise characterization of dielectric materials," *Sci. Rep.*, vol. 9, no. 1, pp. 1-12, 2019.
- [28] Z. Wei, J. Huang, J. Li, G. Xu, Z. Ju, X. Lio, and X. Ni., " ," *Sensors*, vol. 18, no. 11, pp. 4005, Nov. 2018.
- [29] X. Yang, L. Xin, X. Jiao, P. Zhou, S. Wu, and K. Huang, "High-sensitivity structure for the measurement of complex permittivity based on SIW," *IET Sci. Meas. Technol.*, vol. 11, no. 5, pp. 532-537, 2017.
- [30] F. Majeed, T. Fickenscher, M. Shahpari, D. Thiel, "Measurement of surface conductivity of graphene at W-band," *MOTL*, 2019.
- [31] J. Krupka, W. Strupinski, and N. Kwietniewski, "Microwave Conductivity of Very Thin Graphene and Metal Films," *Journal of Nanoscience and Nanotechnology*, 11(4):3358-62, April 2011.
- [32] M. Liang, M. Tuo, S. Li, Q. Zhu, H. Xin, "Graphene conductivity characterization at microwave and THz frequency," *The 8th European Conference on Antennas and Propagation EuCAP*, 2014.
- [33] L. Hao, J. Gallop, S. Goniszewski, O. Shafarost, N. Klein, and R. Yakimova, "Non-contact method for measurement of the microwave conductivity of graphene," *Applied Physics Letters* vol. 103, 123103, doi: 10.1063/1.4821268, 2013.
- [34] G. Moradi and M. Mosalanejad, "Microstrip patch sensors for complex permittivity measurement of medium loss liquids Using 3D-FDTD," *Applied Computational Electromagnetics Society Journal*, vol. 32, no. 4, pp. 325-331, 2017.
- [35] M. Bozzi, A. Georgiadis, and K. Wu, "Review of substrate-integrated waveguide circuits and antennas", *IET Microw., Antennas Propag.*, vol. 5, no. 8, pp. 909-920, 2011.
- [36] Y. Seo, M. U. Memon and S. Lim, "Microfluidic eighth-mode Substrate Integrated-Waveguide antenna for compact ethanol chemical sensor application," *IEEE Trans. Antennas Propag.*, vol. 64, no. 7, pp. 3218-3222, Jul. 2016.
- [37] L. Harrision, M. Ravan, D. Tandel, K. Zhang, T. Patel and R. Amineh, "Material identification using a microwave sensor array and machine learning," *Electronics*, vol. 2, no. 8, pp. 288, Feb. 2020.
- [38] C. Liu and F. Tong, "An SIW resonator sensor for liquid permittivity measurements at C band," *IEEE Microw. Wireless Compon. Lett.*, vol. 25, no. 11, pp. 751-753, Nov. 2015.
- [39] E. Silawve, N. Somjit and I. D. Robertson, "A microfluidic-integrated SIW lab-on-substrate sensor for microliter liquid characterization," *IEEE Sensors J.*, vol. 16, no. 21, pp. 7628-7635, Nov. 2016.
- [40] H. Sun, T. Tang, and G. Du, "Improved approach using symmetric microstrip sensor for accurate measurement of complex permittivity", *Int. J. RF Microw. Comput. Eng.*, vol. 28.5, pp. e21258, 2018.
- [41] D. Deslandes, "Design equations for tapered microstrip-to-substrate integrated waveguide transitions *Proc. IEEE MTT-S Int. Microw. Symp. Digest (MTT)*, pp. 1-1, May. 2010.
- [42] A. Niembro-Martín, V. Nasserddine, E. Pistono, H. Issa, and P. Ferrari, "Slow-wave substrate integrated waveguide," *IEEE Trans. Microw. Theory Techn.*, vol. 62, no. 8, pp. 1625-1633, Aug. 2014.
- [43] A. K. Jha and M. J. Akhtar, "Design of multilayered epsilon-near-zero microwave planar sensor for testing of dispersive materials," *IEEE Trans. Microw. Theory Techn.*, vol. 63, no. 8, pp. 2418-2426, Aug. 2015.
- [44] C. C. Aggarwal, "Neural Network and Deep Learning", Springer, 2018.
- [45] S. Huang, Z. Cao, H. Yang, Z. Shen and X. Deng, "An electromagnetic parameter retrieval method based on deep learning," *J. Appl. Phys.*, vol. 127, no. 22, p. 224902, Jun. 2020.
- [46] M. A. H. Ansari, A. K. Jha, Z. Akhter and M. J. Akhtar, "Multi-band RF planar sensor using complementary split ring resonator for testing of dielectric materials", *IEEE Sensors Journal*, vol. 18, no. 16, pp. 6596-6606, Aug. 2018.
- [47] K. T. M. Shafi, A. K. Jha and M. J. Akhtar, "Improved planar resonant RF sensor for retrieval of permittivity and permeability of materials", *IEEE Sensors Journal*, vol. 17, no. 17, pp. 5479-5486, Sep. 2017.
- [48] G. Moradi and A. Abdipour, "Measuring the permittivity of dielectric materials using stdr approach," *Progress In Electromagnetics Research, PIER* 77, 357–365, 2007.



Gholamreza Moradi received the Ph.D. degree in Electrical Engineering from Amirkabir University of Technology (Tehran Polytechnic), Tehran, Iran in 2002. His main research interests are High Frequency Characterization of Materials, Numerical Electromagnetics, Microwave Imaging, Planar Microwave/MM Wave and THz

Systems. He is conducting some collaborative projects on 5G antenna together with the University of Alberta and the University of Dresden. Dr. Moradi served for almost a decade as a lecturer and research manager in Civil Aviation Technology College. He is currently an Associate Professor with the Department of Electrical Engineering, Amirkabir University of Technology. He has authored over 10 books in his specialty. One of his books was the book of the year of the country in 2008. Gholamreza has published and presented over 200 papers in the refereed journals and international conferences.